International Journal of GEOMATE, July., 2021, Vol.21, Issue 83, pp.-181-190
ISSN: 2186-2982 (P), 2186-2990 (O), Japan, DOI: https://doi.org/10.21660/2021.83.j2105
Geotechnique, Construction Materials and Environment

ESTIMATION OF CARBON DIOXIDE EMISSIONS ON HETEROGENEOUS TRAFFIC BASED ON METROPOLITAN TRAFFIC EMISSIONS INVENTORY MODEL

*Sumarni Hamid Aly[1], Muhammad Isran Ramli[2] and Zulfiani Arifin[3]

[1,2]Faculty of Engineering, Hasanuddin University, Indonesia, [3]Faculty of Engineering, Kupang Polytechnic, Indonesia

*Corresponding Author, Received: 04 Feb. 2021, Revised: 05 Apr. 2021, Accepted: 25 Apr. 2021

ABSTRACT: Traffic on the arterial roads of Makassar City is categorized as heterogeneous traffic and can increase motor vehicle emissions. This study aims to estimate CO_2 emissions from vehicles during morning and evening rush-hour traffic on nine arterial roads. This study used the MARNI model approach, which is a prediction model of vehicle emissions in heterogeneous traffic based on moving vehicles, and adapted it to the International Vehicle Emission Model (IVEM). The four factors that are considered to predict vehicle emissions are emission factors, driving cycle as a reference for vehicle speed, vehicle operational characteristics, and travel time. As a result, from 31 vehicle categories, the highest CO_2 emissions are CV_{24}: MPFI, 3 Way/EGR, Medium, and 0–6 years. The highest and lowest vehicle volumes and total CO_2 emissions occurred on the RD3 and RD5 roads, respectively. This indicates a linear correlation between the vehicle volume and the levels of CO_2 emissions. For future studies, the MARNI model can be used as a reference for predicting the emissions of motorcycles and heavy vehicles.

Keywords: Arterial road, Heterogeneous traffic, CO_2 emissions, Marni model

1. INTRODUCTION

Currently, the transportation sector contributes majorly to the increase in greenhouse gas emissions [1]. Consequently, the increase in pollutant emissions has a potential effect on human health, the economy, and society [2]. Globally, vehicle numbers have been predicted to increase ten-fold by 2050 [3]. Furthermore, road transport accounts for 74% of CO_2 emission from transportation [4]. Moreover, the amount of motor vehicles has increased CO_2 and NOx emissions by 7% and 11%, respectively [5,6]. Thus, the evaluation and control of CO_2 emissions generated from traffic in urban areas should be considered [6,7].

Emission reduction is one of the fundamental issues in solving problems related to global warming and climate change [8,9]. Because a significant portion of the emissions comes from transportation, especially from ground vehicles, it is suggested that the reduction of emissions should be taken into consideration when road administrators plan road traffic controls. Therefore, it is important to improve the quality of traffic emission inventory with more accurate estimates of total vehicle emissions [7].

The International Vehicle Emission Model [10] is a reference model for estimating motor vehicle emissions. The IVEM is built based on homogeneous and stable traffic flow conditions and is used to estimate emission levels in developing countries [10,11]. The model has been widely applied to minimize pollution by motor vehicles operating on highways, tolls, arteries or collector roads, and local roads. Additionally, this model considers four components: the operational character of the vehicle, the real driving cycle on the road, vehicle travel time, and vehicle emission factors [10-14]. For vehicle with gasoline, diesel, and other fuels, the emission factors must be corrected for both temperature and humidity [15,16].

Motor vehicles are divided into light vehicles, heavy vehicles, buses, and motorbikes [1,2,17,18]. The first component that has a significant effect on vehicle emissions is the operational characteristics of the vehicle, which consists of, type of exhaust, type of engine, vehicle engine capacity, vehicle age, and length of vehicle trip [10,15,19-21]. The second component is the vehicle driving cycle pattern. In Indonesia, which is a developing country, the traffic flow is heterogeneous; meanwhile, in developed countries, the traffic flow is homogeneous. Therefore, the vehicle driving cycle pattern is different from that of developed countries. Previous studies have revealed that heterogeneous traffic has certain characteristics, such as traffic flow or inconsistent vehicles on lane roads, and inconstant vehicle speeds [22-24]. Hence, travel time and vehicle speeds fluctuate significantly with different types of vehicles operating on the road simultaneously. To adopt and adapt the IVEM for heterogeneous traffic flows with unstable vehicle speeds, it is necessary to adjust the driving cycle patterns, emission factors, and vehicle travel time [23-25]. The third component, which is vehicle travel time, is also unstable and fluctuates owing to c unstable vehicle speeds. Meanwhile, the fourth component that is the emission factor, which has a significant effect on total vehicle emissions on the road, was analyzed as basic emissions per vehicle of categories [10,26]. This study aims to estimate the total carbon dioxide (CO_2) emissions on arterial roads from 31 light vehicle volume categories, using the MARNI model by considering the driving cycle patterns, operational characteristics, vehicle emission factors, and vehicle travel times in Makassar City.

2. RESEARCH SIGNIFICANCE

Here, a model of driving cycle patterns and vehicle emission factors was developed using a 3rd degree polynomial model. The driving cycle is divided into 13 fractions as a representation of heterogeneous traffic flow, whereas the model of 31 emission factors was established from 31 vehicle categories. The vehicle categories were obtained from eight types of exhaust, two types of vehicle engines, two sizes of vehicle engines, and three vehicle model year classifications. Furthermore, a travel time model was built using a non-linear regression model with an independent variable, the length of the road, the number of lanes, and the type of intersections along the road.

3. EXPERIMENTAL METHODS

In previous studies, researchers have studied environmental pollutants taking various approaches. The IVEM was used as a prediction model developed by the International Sustainable Systems Research Center and the University of California, Riverside [10,27].

In addition, this model can be applied to measure the amount of pollution from vehicles at both macro and micro levels. The primary data consist of traffic characteristics, traffic behavior patterns, and emission factors based on local conditions.

3.1 Heterogeneous Traffic Analysis

The first stage of the Metropolitan Traffic Emissions Inventory Model (Marni Model) is the analysis of the heterogeneous traffic flow as a method to predict the vehicle emissions [23,24]. The second stage is to analyze macro traffic characteristics, which are vehicle volumes and vehicle speeds. The third stage analyzes the operational characteristics of the vehicle. These categories consist of the type of engine technology (t), engine size (c), exhaust type (ET), vehicle age (a), and vehicle fuel consumption [10,19]. The measured variables in this study are shown in Table 1.

Table 1 Measured variables in heterogeneous traffic analysis

Flow of heterogeneous traffic	Measured variables
Heterogeneous vehicle type [17,18]	1. Motor vehicle: Motorcycle (MC), Light vehicles (LV), and Heavy vehicles (HV) 2. Non-motorized vehicle
Characteristic of operational vehicle [10,15,19-21]	1. Exhaust type/ET (3-way, 3-way/EGR, SULEV, ULEV) 2. Vehicle engine type/t (Carburetor, Multipoint Fuel Injection /MPFI) 3. Engine capacity/c (light < 1500 cc, medium 1500-2000 cc, and heavy >2000cc) 4. Length of vehicle trip (can be seen from odometer) 5. Fuel types (gasoline, diesel)
Macro characteristics of traffic flow [17]	1. Vehicle volume 2. Vehicle speed
Age of vehicle on the roads [10,13,20,21]	The age of vehicles (a) are classified according to the IVE Model (provided in the letter of vehicle ownership) 1. 0 – 6 years; 2. 6 - 13 years; 3. >13 years
Driving cycle of vehicle flow [23-25]	Driving cycle (DC) indicates a fraction of vehicle speed (V) from 0-60 km/h. The V fraction is distributed into 13 classifications, such as $V_1=0$, $V_2=5$, $V_3=10$, $V_4=15$, $V_5=20$, $V_6=25$, $V_7=30$, $V_8=35$, $V_9=40$, $V_{10}=45$, $V_{11}=50$, $V_{12}=55$, and $V_{13}=60$

3.2 Vehicle Categories Based on Operational Characteristics

The vehicles were categorized based on their operational characteristics to measure the total emissions, as presented in Table 1. The vehicle operational characteristics were obtained by conducting interviews with vehicle owners at the study locations.

By mapping the operational characteristics of the vehicle, we obtained the vehicle categories, as listed in Table 2.

Table 2 Categories of vehicle (CV) mapping

Exhaust type (ET)	Type of vehicle engine (t)											Total CV_N (unit)
	Light size			Medium size		Light size			Medium size			
	0-6	6-13	>13	6-13	>13	0-6	6-13	>13	0-6	6-13	>13	
ET_1	$CV_{1.1}$	$CV_{1.2}$	$CV_{1.3}$	$CV_{1.4}$	…	…	…	…	…	…	$CV_{1.11}$	ET_{N1}
ET_2	…	…	…	…	…	…	…	…	…	…	…	ET_{N2}
.	…	…	…	…	…	…	…	…	…	…	…	.
.	…	…	…	…	…	…	…	…	…	…	…	.
ET_m	$CV_{m.1}$	CV_m	$CV_{m.3}$	CV_m	…	…	…	…	…	…	$CV_{m.11}$	ET_{Nm}
Total CV_N (Unit)	$CV_{1\text{-}m}$	…	…	…	…	…	…	…	…	…	$CV_{11\text{-}m}$	CV_N= ET

Table 2 shows that each cell is a representation of the volume of the vehicle category (CV_i) according to ET, engine type (t), vehicle engine capacity (c), and vehicle age (a). The total vehicle volumes (CV_N) are the result of all vehicle category cells at rush-hours of 7:00 - 8:00 (AM) and 16:00 - 17:00 (PM) [2], which can be analyzed as shown in Eq. (1) and Eq. (2).

$$CV_{N(t,c,a,e)} = ETi = f\{\text{Vehicle Volume}\} \tag{1}$$

$$CV_{N(t,c,a)} = \begin{bmatrix} CV_{1.1} & CV_{1.2} & \dots & CV_{1.11} \\ CV_{2.2} & CV_{1.2} & \dots & CV_{2.11} \\ \dots & \dots & \dots & \dots \\ \dots & \dots & \dots & \dots \\ CV_{m.1} & \dots & \dots & CV_{m.11} \end{bmatrix} \tag{2}$$

The vehicle volume based on ET was calculated using Eq. (3).

$$\begin{aligned} ET_{N1} &= CV_{1.1} + CV_{1.2} + \dots + CV_{1.11} \\ ET_{N2} &= CV_{2.1} + CV_{3.2} + \dots + CV_{2.11} \\ &\vdots \\ ET_{Nm} &= CV_{m.1} + CV_{m.2} + \dots + CV_{m.11} \end{aligned} \tag{3}$$

$CV_{N(t,c,a)}$ can be also formulated into Eq. (4).

$$CV_{N(t,c,a)} = ET_i = ET_{N.1} + \dots + ET_{N.m}\,; \tag{4}$$

i = 1,2,3, ….. , n)

3.3 Vehicle Volume Measurement

The vehicle volume was determined directly from a direct survey conducted on the road using a camera video. This research was conducted on nine arterial roads in Makassar City (Fig. 1):

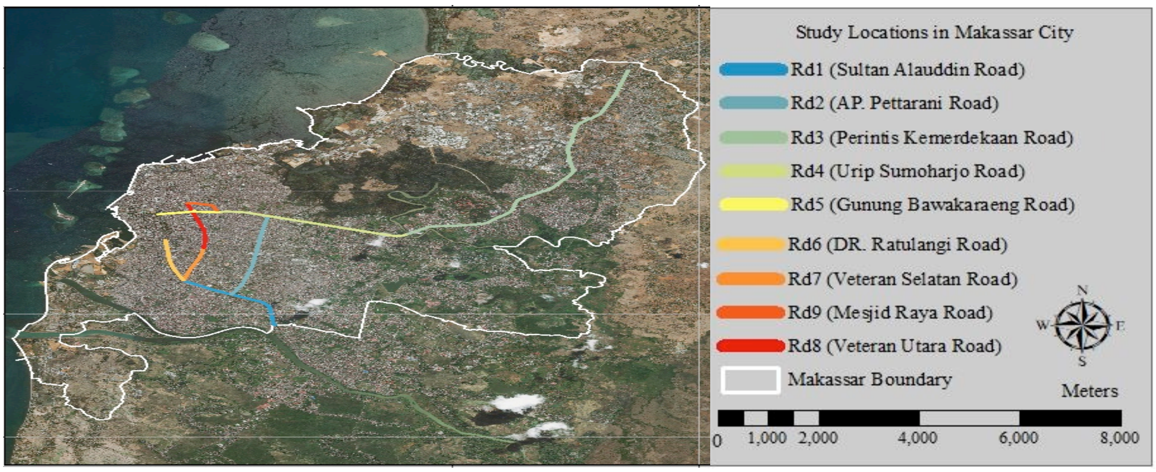

Fig.1 Locations of study

As shown in Fig. 1, the nine roads are Sultan Alauddin road (Rd1), AP. Pettarani road (Rd2), Perintis Kemerdekaan road (Rd3), Urip Sumoharjo road (Rd4), Gunung Bawakaraeng road (Rd5), DR. Ratulangi road (Rd6), Veteran Selatan road (Rd7), Veteran Utara road (Rd8), and Mesjid Raya road (Rd9). For Rd5 and Rd9, the vehicle volume was observed in only one direction of the traffic flow, whereas for others observations were made in both directions. The road areas consist of the central business district and the urban area of Makassar City. These roads are arterial roads and have a significant role in transporting goods and people from and to the central business districts (CBD).

3.4 Estimation of Carbon Dioxide Emission from Moving Vehicles on the Highway

3.4.1 Metropolitan traffic emissions inventory (MARNI) model

The total CO_2 emissions from the emission vehicle (EV) have been incorporated into the MARNI model [13], which is a multiplication of vehicle volume (N), emission factor (EF), parameters of average-speed fraction distribution (DC), and travel time (TT), as shown in Eq. (5).

$$EV^{t}_{(i,p)} = N \times EF_{(i,p)} \times DC^{t} \times TT^{t} \quad (5)$$

Index of t on Eq. (5) is the survey period, i is the vehicle category, and p is the type of pollutant estimated. In this study, we defined CO_2 as a pollutant. For several vehicle categories, the EV can be formulated as shown in Eq. (6), which is similar to Eq. (5), where $N = CV^{t}_{i}$.

$$EV^{t}_{(i,p)} = \sum_{i=1}^{n} CV^{t}_{i} \left(EF_{(i,p)} \text{ x } DC^{t} \text{ x } TT^{t} \right); \quad (6)$$
i= 1, 2, 3, …, n

3.4.2 Model of driving cycle (DC) and TT

The driving cycle model is called 3T-0-60 [13]. This model refers to the vehicle speed from 0 km/h (the engine on while the vehicle not moving) to 60 km/h. According to [17], 60 km/h is the determined speed limit on arterial roads. Because of the fluctuating vehicle speeds, which are influenced by acceleration, deceleration, and idle, the vehicle speed (DC) and TT were distributed into 13 fractions [12,22,25,28].

Hence, the distributions of the DC and TT are classified into 13 fractions for all directions of moving vehicles in the morning (a) and afternoon (p) periods, as shown in Table 3.

Table 3 Distribution of driving cycle (DC) and TT

No	Speed (V_1-V_{13}) km/h	Driving Cycle Distribution (%)				TT (h)	
		Direction A		Direction B		Direction A	Direction B
		AM	PM	AM	PM		
1	0	$DC^{1}_{i=1}$	$DC^{1}_{j=1}$	$DC^{2}_{i=1}$	$DC^{2}_{j=1}$	$TT^{1}_{i=1}$	$TT^{2}_{i=1}$
2	5	...	...	...	...	...	...
3	10	...	...	...	...	$TT^{1}_{i=3}$	$TT^{2}_{i=3}$
4	15	$DC^{1}_{i=4}$	$DC^{1}_{j=4}$	$DC^{2}_{i=4}$	$DC^{2}_{j=4}$	...	...
5	20	...	...	...	...	...	...
6	25	...	...	...	...	$TT^{1}_{i=6}$	$TT^{2}_{i=6}$
7	30	$DC^{1}_{i=7}$	$DC^{1}_{j=7}$	$DC^{2}_{i=7}$	$DC^{2}_{j=7}$	...	...
8	35	...	...	...	...	...	...
9	40	...	...	...	...	$TT^{1}_{i=9}$	...
10	45	...	...	...	...	...	...
11	50	...	...	...	...	...	...
12	55	...	...	...	...	...	...
13	60	$DC^{1}_{i=13}$	$DC^{1}_{j=13}$	$DC^{2}_{i=13}$	$DC^{2}_{j=13}$	$TT^{1}_{i=13}$	$TT^{2}_{i=13}$
Σ		DC^{1}_{AM}=100	DC^{1}_{PM}=100	DC^{2}_{AM}=100	DC^{1}_{PM}=100	TT^{1}	TT^{2}

Additionally, the vehicle volume and TT assumed did not change during those times [6].

Index numbers V_1 - V_{13} are the fractions of vehicle speed 0-60 km/h; meanwhile, i and j are the values associated with the DC in the AM and PM periods, respectively. Meanwhile, DC^1 and DC^2 indicate the DC values in directions A and B.

According to [13], DC can be expressed as Eq. (7) and Eq. (8).

$$\left. \begin{aligned} DC^{1}{}_{AM} &= \sum_{i=1}^{13} DC^{1}{}_{i} = 100\% \\ DC^{1}{}_{PM} &= \sum_{j=1}^{13} DC^{1}{}_{j} = 100\% \end{aligned} \right\} \quad (7)$$

$$\left. \begin{aligned} DC^{2}{}_{AM} &= \sum_{i=1}^{13} DC^{2}{}_{i} = 100\% \\ DC^{2}{}_{PM} &= \sum_{j=1}^{13} DC^{2}{}_{j} = 100\% \end{aligned} \right\} \quad (8)$$

Moreover, the TT was derived from the mathematical formula of the light vehicle (LV) with heterogeneous traffic flow on the main road in Makassar City [29], as shown in Eq. (9).

$$TT = 202.759 + 0.095(JP) - 31.355(JL) + 14.126(JSB4B) + 2.332(JS3B) \quad (9)$$

where TT is the total travel time, JP is the distance the vehicle is moving, JL is the number of lanes on the road, JS4B is the intersection type 4, and JS3B is the type of intersection 3. JP is then elaborated according to the 13 fraction cycles of the DC. Furthermore, the travel time per vehicle category is analyzed as the result of multiplying the DC and total TT, as shown in Table 3, and can be written as Eq. (10).

$$TT^1{}_{i=1} = f(DC^1{}_{i=1}) \times TT^1; TT^1 = \sum_{i=1}^{13} TT^1{}_{i=1} \quad (10)$$

Equation (11) can also be written in matrix form, as shown in Eq. (11).

$$\begin{pmatrix} TT^1{}_{i=1} \\ TT^1{}_{i=2} \\ \ldots \\ TT^1{}_{i=12} \\ TT^1{}_{i=13} \end{pmatrix} = \begin{pmatrix} DC^1{}_{i=1} \\ DC^1{}_{i=2} \\ \ldots \\ DC^1{}_{i=12} \\ DC^1{}_{i=13} \end{pmatrix} \times TT^1 \quad (11)$$

3.4.3 EF in MARNI model

Several models of EFs have been developed by researchers in previous studies [26,30,31]. For instance; 1) "Average-speed' models (e.g., COPERT, MOBILE, EMFAC), in which EFs (in g veh./km) are a function of the mean traveling speed; 2) 'Traffic-situation' models (e.g., HBEFA, ARTEMIS), in which descriptions of a particular traffic situation determines the EFs (in g veh./km) (e.g. 'stop-and-go-driving," 'free flow motorway driving'); and 3) 'Cycle-variable' models (e.g., MEASURE, VERSIT), in which EFs (in g veh./km or g/s) are functions of various driving cycle variables (e.g., idle time, average speed, positive kinetic energy) at high resolution (seconds to minutes).

However, vehicle EFs fluctuate because of many factors, particularly traffic conditions and driving cycles of the driver behavior. Therefore, the base vehicle emission values will be different from one road, area, city, or region to another [13]. The MARNI model EF was developed based on the base EF of IVEM (g/h). The factor was defined using a function of vehicle speed, which was a 3rd order polynomial [11], as shown in Eq. (12).

$$EF_{(i,p)} = \beta_0 + \beta_1 V^1 + \beta_2 V^2 + \beta_3 V^3 \quad (12)$$

where EF is the emission factor, i is the vehicle category, p is the pollutant, V is the vehicle speed, β_0 is a constant, and β_1, β_2, and β_3 are parameter models, as shown in Table 4.

Table 4 The matrix of Emission Factors (EF)

EF_i	Parameter model EF			
	β_0	β_1	β_3	β_4
EF_1	a_1	b_1	c_1	d_1
EF_2	a_2	b_2	c_2	d_2
…	…	…	…	…
EF_{31}	a_{31}	a_{31}	c_{31}	d_{31}

Furthermore, a is a generic value of the constant β_0. The values of β_1, β_2, and β_3 for each vehicle category (CV) are b, c, and d. Moreover, the i is the category index (1,2,3,... 31). The CO_2 EFs of the 31 vehicle categories are elaborated from five types of vehicle technology by adapting the adjustment factors to the IVEM EFs, as shown in Fig. 2.

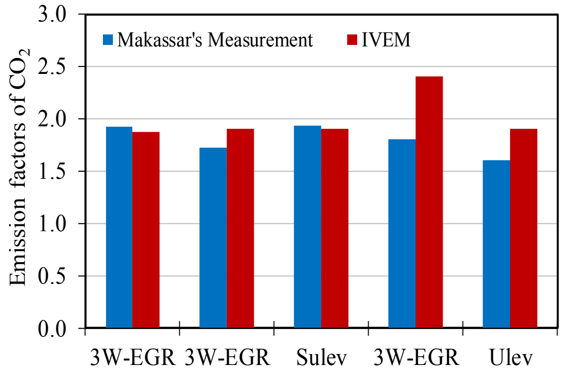

Fig.2 EF of Marni Model and IVEM

The EF of CO_2 corresponds to the EF value of the IVEM for all vehicle types, excluding the vehicle type of three-way/EGR and ULEV. These types have lower EF values than the IVEM.

3.4.4 Relation of EF and driving cycle

Furthermore, the result of the multiplication between the EF and the vehicle speed is indicated by the distribution of the driving cycle, as shown in Eq. (12), and can be rewritten as Eq. (13).

$$EF = \sum_{i=1}^{n} EF_{i,p}; \left. \begin{matrix} EF_{i,p} = EF_1 \\ EP_{i,p} = EF_2 \\ \ldots \\ \ldots \\ EP_{i,p} = EF_n \end{matrix} \right\} \text{For } DC_1,..,DC_{13} \quad (13)$$

Besides, Eq. (13) can be rewritten as Eq. (14) according to the vehicle speed in Table 3, and EF models a, b, c, and d, as seen in Table 4.

Then, EF_1, EF_2, ..., EF_{31} can becalculated using Eq. (14).

$$EF_1 = \left.\begin{matrix} a_1 + b_1DC_1 + c_1DC_1 + d_1DC_1 \\ a_1 + b_1DC_2 + c_1DC_2 + d_1DC_2 \\ \dots \\ \dots \\ a_1 + b_1DC_{13} + c_1DC_{13} + d_1DC_{13} \end{matrix}\right\} \quad (14)$$

4. RESULTS AND DISCUSSION

According to vehicle volume data (2010-2014) and vehicle categories in Table 2, we obtained 31 categories of eight types of exhaust, two types of vehicles engines, two vehicle engine sizes, and three vehicle age classifications. The eight exhaust types of vehicles classified based on [10] were 3way, 3way/EGR, Euro 3, Hybrid, None, SULEV, ULEV, and Euro 4. Two types of vehicle engines were carbureted and multipoint fuel injection (MPFI). The vehicle engine size was classified into medium and light, and vehicle age was classified into 0-6 years, 6-13, and > 13 years [13].

4.1 Vehicle Volume of 31 Categories

The bar chart (Fig.3) depicts the volume distribution of 31 vehicle categories with different measuring periods: morning (a) and afternoon (b).

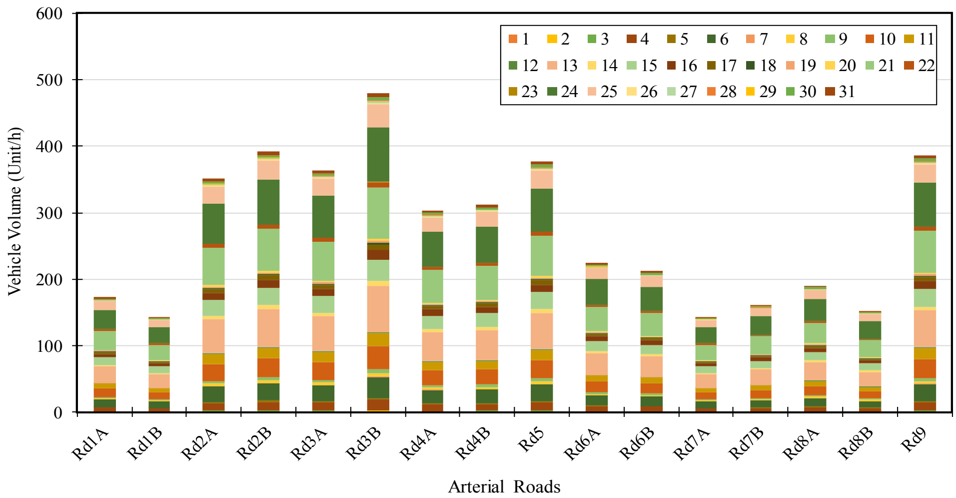

(a)

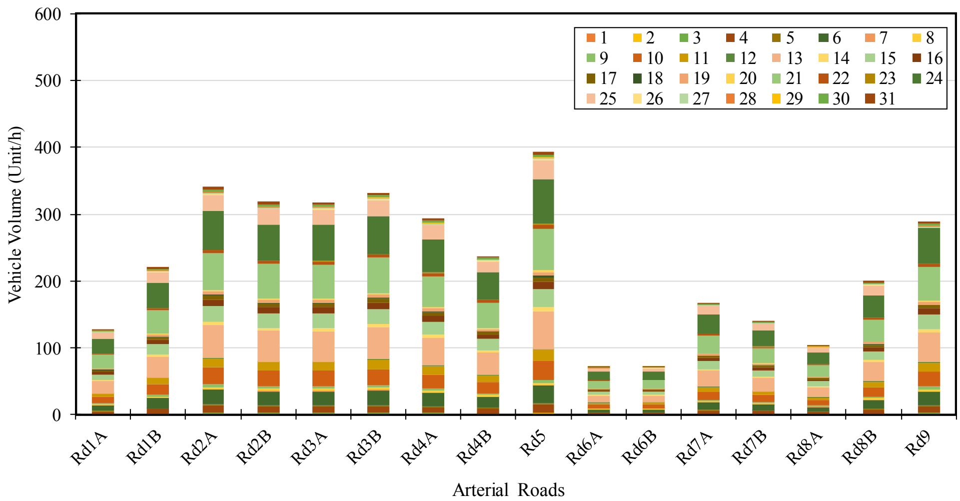

(b)

Fig.3 Vehicle Volume on Arterial Roads based on 31 categories of vehicles (CV). (a) Vehicle Volume on the morning (b) Vehicle Volume on the afternoon

As a result, the vehicle volume is more significant in the morning for directions A and B. The largest vehicle volume in the morning period was recorded on Rd3 (Rd3A + Rd3B) with 851 units/h. The lowest value was found on Rd7 (Rd7A + Rd7B) with 308 units/h. Furthermore, the high and low rates of volume distribution in the afternoon periods were at Rd2 (Rd2A + Rd2B) with 659 units/h, and Rd6 (Rd6A + Rd6B) with 144 units/h, respectively (Fig. 3a and Fig. 3b).

The dominant category of vehicles was CV_{24}, with the following operational characteristics: MPFI, 3 Way/EGR, Medium, 0–6 years, located on Rd5 of 67 units/h.

4.2 Driving Cycle and TT

The TT and vehicle speed distribution fraction (DC) were determined using Eqs. (11) and then elaborated in Eq. (12). For instance, the results of the driving cycle distribution and TT for AM and PM in Rd1 are shown in Fig. 4.

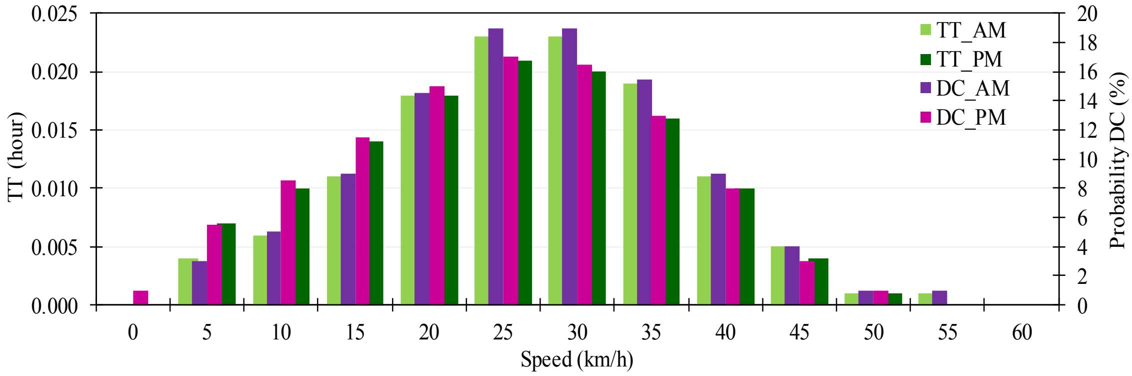

Fig.4 Speed, driving cycle, and TT

Fig. 4 describes the results of the DC and TT distributions at different times and is classified into 13 classes in RD1. As illustrated in the morning rush-hour, the DC distribution fraction dominated at 25–30 km/h (19%).

Meanwhile, for the afternoon hour, 17% of the driving cycle distribution was at 30 km/h. This condition shows that the performance of RD1 has decreased by 50% from the planned of speed of 60 km/h. In addition, the idle condition was not observed in the morning. Contrarily, in the afternoon, a 1% idle condition was found.

The dominant speed was 55–60 km/h during the PM. This indicates that the traffic condition was more crowded and jammed in the afternoon than it was in the morning. Traffic condition is distributed in the same DC in AM and PM, for total TT values of 0.122 and 0.121 h, respectively.

4.3 EFs of Carbon Dioxide

The EFs of CO_2 for the 31 vehicle categories (CV) are shown in Fig. 5. It states that some factors have similar values.

These EFs were divided into two groups: vehicles with carbureted engines, $CV_1 \sim CV_7$, and vehicles with MPFI engines, $CV_8 \sim CV_{31}$. Some factors have similarities, such as CV_8 with CV_9, CV_{10}, CV_{11}, and CV_{12}, CV_{13}, $CV_{14,}$ and CV_{15} with CV_{16}. These similarities indicate the same type of engine and exhaust. Among all vehicle categories, CV_{10}, $CV_{11,}$ and CV_{12} have the highest EFs of CO_2. Based on the engine types, the vehicle's EF of the MPFI engine is higher than the carbureted type, which is 3.800–7.500 g/h and 900–1.900 g/h, respectively.

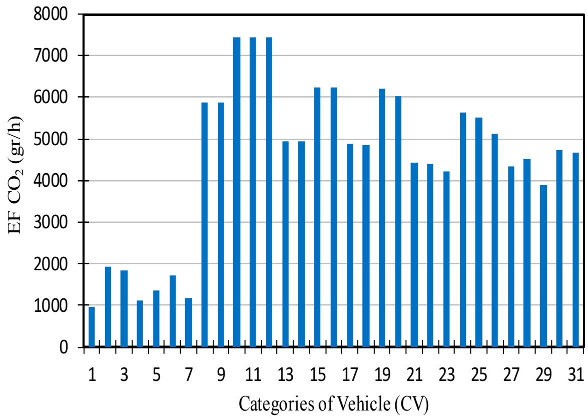

Fig.5 CO_2 EFs for 31 CV

4.4 Prediction of CO_2 Emission

4.4.1 Estimation of CO_2 Emission per Vehicle Category

CO_2 emissions are mainly based on the engine type. As a result, MPFI CO_2 emissions are greater than those of carbureted engines for all directions in the AM and PM periods. The total CO_2 emissions for MPFI engines are between 0.013 tons and 0.024 tons, while for carbureted engines, it is between 0.00003 tones and 0.0001 tones.

For the A direction, the largest CO_2 emission occurred at 0.018 tons in the AM time. Meanwhile, the highest in the B direction was 0.024 tons in the PM period. Moreover, the highest and lowest CO_2 emissions for each vehicle category in the PM periods were derived from CV24 (MPFI, 3 Way/EGR, Medium, 0–6 years) of 0.024 tones, and CV21 (MPFI, 3 Way/EGR, Light, 0–6 years) of 4.95 x10-6 tones, as illustrated in Fig. 6

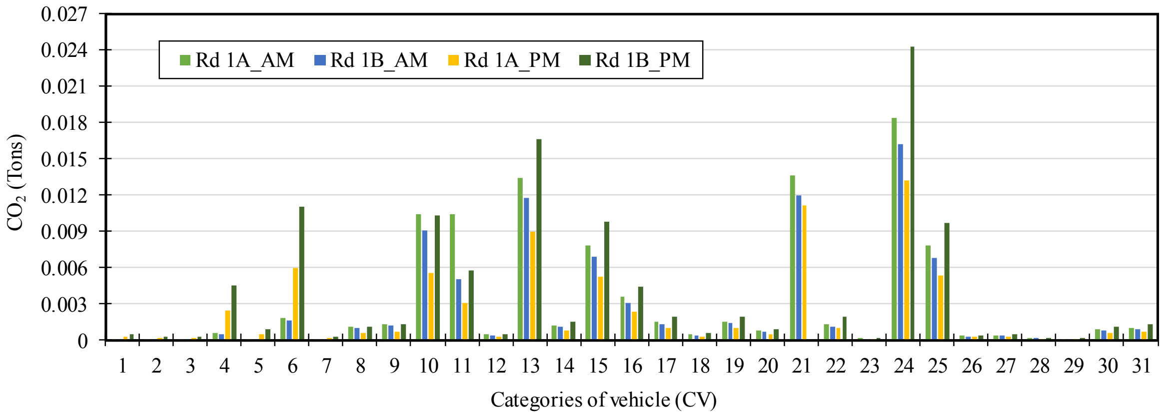

Fig.6 CO_2 emissions for 31 categories of vehicles in Rd1 for both directions A and B

4.4.2 Prediction of CO_2 Emission Total on Arterial Road

The predicted total CO_2 emissions from 31 types of category vehicles on nine arterial roads are shown in Fig.7. Emission CO_2 was in the range of 0.05 ton-1.52 ton and 0.03 ton-1.05 ton during morning and afternoon, respectively. According to the statistical t-test, the amount of CO_2 in AM and PM periods are different with variance, t-critical 2.31 > t-statistic 1.47.

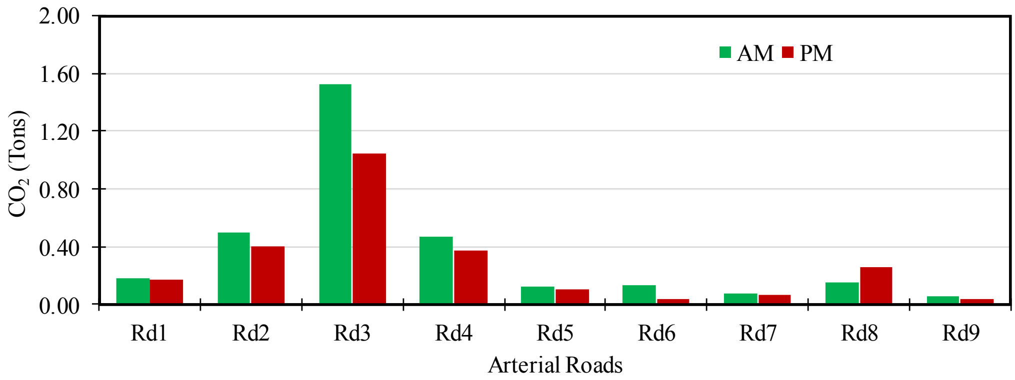

Fig.7 CO_2 emissions on arterial roads Rd1-Rd9

The total emissions show that most CO_2 emissions occurred in the AM rather than in the PM period outside RD8. This condition indicates that vehicles moved simultaneously in the morning because of this road being the center of mobilization for urban activities such as work, school, campus, etc.

The total emissions were found on Rd2, Rd3, and Rd4 among the nine other roads. This was caused by the large volume of vehicles. Rd2 is an access road connecting cities in the North to Makassar City. Meanwhile, Rd3 and Rd4 are non-toll roads, which are accessibility points from the city of Makassar to the airport, and the exit roads from this city to the east and north of Makassar City.

From these roads, the largest emission is on Rd3 in the morning with 1.52 ton, and the lowest emission is on Rd9 in the afternoon with 0.03 tons. Previous researchers [32] stated that the largest CO_2 emissions occurred on Rd3 as well.

5. CONCLUSION

The CO_2 emissions are estimated in this study according to the Metropolitan Emissions Inventory (MARNI) in Makassar City with heterogeneous traffic conditions. This model is analyzed with four variables: EFs, vehicle driving cycle (speed), vehicle operational characteristics, and TT.

The EF of CO_2 was adapted from the basic EF of IVEM.

Moreover, the driving cycle and TT were divided into 13 classes as a reference for fluctuating vehicle speeds, which is one of the characteristics of heterogeneous traffic. In addition, vehicle volume was categorized into 31 categories based on the operational characteristics of the vehicle, which is also referred to by IVEM. The highest and lowest vehicle volumes were located in Perintis Kemerdekaan (Rd3) and Mesjid Raya (Rd5), respectively.

Moreover, the highest and speed values represent the highest results in the AM compared to PM periods. This indicates that traffic has congested in the PM time. The highest total CO2 emissions occurred on the Perintis Kemerdekaan road (Rd3), and the lowest emissions were located on the Mesjid Raya road (Rd5) from the nine arterial roads in Makassar City. This indicates that the volume of vehicles is directly proportional to the emissions emitted by motor vehicles.

In a future study, the MARNI model can be referenced for the development of vehicle driving cycle and EFs of motorbikes and heavy vehicles in Makassar City, as well as studying the relationship between vehicle speed and road slope.

6. ACKNOWLEDGMENTS

The author would like to thank the Laboratory of Traffic Engineering, Engineering Faculty, Hasanuddin University, for granting access to traffic volume databases.

7. REFERENCES

[1] Pornsuda P., Hathairattana G. and Sopa C., Black Carbon in PM 2.5 at Roadside Site in Bangkok, Thailand. International Journal of Geomate, Vol.19, Issue 72, 2020, pp. 81-87.
[2] Thanapol P., Thaned S. and Wichuda S., Vehicle Actuated Signal Control for Low Carbon Society. International Journal of Geomate, Vol.16, Issue 55, 2019, pp. 86-91.
[3] Amin, N., Reduction Emissions from Private Cars: Incentive measures for behavioral change. United Nations Environment Programme, 2009.
[4] Metz B., Davidson O. R., Bosch P. R., Dave R., Meyer L. A., Climate Change: Mitigation. Contribution of Working Group III to the Fourth Assessment Report of the Intergovernmental Panel on Climate Change. Cambridge Univ. Press, UK, 2007.
[5] Hwang K.P. and Tseng P., CO_2 Emission: Status, Reduction Policy, and Management Strategy of Taiwan's Transportation Sector. Proc. 7th International Conference of The Eastern Asia for Transportation Studies, September 05, 2007, Dalian, China: Vol. 6.
[6] Chang C.T. and Lin T.P., Estimation of Carbon Dioxide Emissions Generated by Building and Traffic in Taichung City. Sustainability, Vol. 10, Issue 1, 2018, pp. 1-18.
[7] Deng F., Lv Z., Qi L., Wang X., Shi M., and Liu H., A big data approach to improving the vehicle emission inventory in China. Nature Communications, Vol. 11, 2020, pp. 1-12.
[8] Liu H., Fu M., Jin X., Shang Y., Shindell D., Faluvegi G., Shindell C., and He K., Health and climate impacts of ocean-going vessels in East Asia. Nat. Clim. Change Vol. 6, 2016, pp. 1037–1041.
[9] Hata H. and Tonokura K., Impact of next-generation vehicles on tropospheric ozone estimated by chemical transport model in the Kanto region of Japan. Sci. Rep., Vol. 9, 2019, pp. 1–8.
[10] IVE Model, User's Guide, Model, and Data Files, 2004, [Online], retrieved from http://www.issrc.org. [Accessed: 30 July 2010]
[11] Aly, S. H. and Ramli M. I., A Development of MARNI 12.2 Model: A Calculation Tool of Vehicular Emission for Heterogeneous TrafficConditions. Journal of Engineering and Applied Sciences, Vol. 11 Issue 1, 2016, pp. 43-50.
[12] Nesamani K.S. and Subramanian K.P., Development of a Driving Cycle for Intra-City Buses in Chennai, India. Atmospheric Environment, Vol. 45, Issue 31, 2011, pp. 5469-5476.
[13] Aly, S.H., The Emissions of Transportation. 1st ed. Jakarta, Indonesia, Penebar PLUS+, ch. III & IV, sec. A. 1., 5, E. 2a; 2015, pp. 44–92.
[14] Haikun W., Chen C., Huang C., and Fu L., On-road Vehicle Emission Inventory and Its Uncertainty Analysis for Shanghai, China. Science of the Total Environment, Vol. 398, Issue 1-3, 2008, pp. 60-67.
[15] Lents J.M., Osses M., Davis N., and Nikkila N., Comparison of On-road Vehicle Profiles Collected in Seven Cities Worldwide. Proc. 13th International Symposium Transport and Air Pollution, September 13-15, 2004, Boulder, Colorado, USA.
[16] Lents J., Canada M., Nikkila N., Tolvett S., Measurement of In-Use Passenger Vehicle Emissions in Almaty, Kazakhstan, 2007.
[17] DGoH (Directorate General of Highways), 1997. Indonesian Road Capacity Manual (MKJI). Jakarta, Ministry of Public Works.
[18] Gowri A., Object-oriented Methodology for Intersection Simulation Model Under Heterogeneous Traffic Conditions. Advances in Engineering Software, Vol. 40, 2009, pp. 1000-1010.
[19] Park A., Lee J., and Lee C., State-of-the-art Automobile Emissions Models and Applications in North America and Europe for Sustainable Transportation. KSCE Journal of Civil Engineering, Vol. 20, Issue 3, 2016, pp. 1053-1065.
[20] Hui G., Qing-yu Z., Yao S., and Da-hui W., Evaluation of the International Vehicle Emission (IVE) model with on-road remote sensing measurements. Journal of Environmental Sciences, Vol. 19, 2007, pp.

818–826.
[21] Lasmini A. and Amelia K.I., Improvement of Public Transport to Minimize Air Pollution in Urban Sprawl, International Journal of Geomate, Vol. 17. Issue 59, 2019, pp. 43-50.
[22] Arasan V.T., Methodology for Determination of Concentration of Heterogeneous Traffic. Journal of Transportation Systems Engineering and Information Technology, Vol. 10, Issue 4, 2010, pp. 50-61.
[23] Tamsanya N. and Supachart C., Influence of Driving Cycles on Exhaust Emissions and Fuel Consumption of Gasoline Passenger Car in Bangkok. Journal of Environmental Sciences, Vol. 21, Issue 5, 2009, pp. 604-611.
[24] Qian-qian T., Jing-jie C., and Jian-kang D., A Method of Constructing the Fuel Efficiency Model Based on Quadratic Polynomial Regression. Procedia Engineering Vol. 15, 2011, pp. 3749-3753.
[25] Lipar P., Strnad I., Česnik M., and Maher T., Development of Urban Driving Cycle with GPS Data Post Processing Promet-Traffic &Transportation, Vol. 28, Issue 4, 2016, pp. 353-364.
[26] Robin S., Leonidas N., and Paul B., Validation of Road Vehicle and Traffic Emission Models and Meta-Analysis. Atmospheric Environment, Vol. 44, 2010, pp. 2943-2953.
[27] CARB, California Air Resources Board EMFAC Model, 2004, [Online], retrieved from www.arb.ca.gov/msei. [Accessed: 30 July 2010].
[28] Wang Q., Huo H., He K., Yao Z., and Zhang Q., Characterization of Vehicle Driving Patterns and Development of Driving Cycles in Chinese Cities. Transportation Research, Part D, Vol. 13, 2008, pp. 289-297.
[29] Hasrul M. R., Aly S. H., and Ramli M. I., The Analysis of The Time Travel of Light Vehicles on The Arterial Roads, Makassar City. Civil Engineering Departement, Repository Hasanuddin University, Makassar, Indonesia, 2013.
[30] Smith R., Characterization of Urban Commuter Driving Profiles to Optimize Battery Size in Light-Duty Plug-in Electric Vehicles. Transportation Research, Part D, Vol. 16, 2011, pp. 218-224.
[31] Al-Thani H., Koç M., Fountoukis C., and Isaifan R. J., Evaluation of particulate matter emissions from non-passenger diesel vehicles in Qatar. Journal Of The Air & Waste Management Association, Vol. 70, Issue 2, 2020, pp. 228–242.
[32] Elfina A., Analysis of Pollutant Level on Several Main Street In Makassar City. Environmental Engineering Departement, Repository Hasanuddin University, Makassar, Indonesia, 2013.